Performance Evaluation and Mechanism Exploration of Heavy Metal Ion Adsorption by Four Carbon Materials

[1]Songhui Liu, [2]Ting Wang*, [3]Weize Sun, [2]Jingle Chen, [2]Huali Chen
[1]*Hangzhou Vocational & Technical College, Hangzhou, Zhejiang 310018, China.*
[2]*School of Environmental Science and Engineering, Zhejiang Gongshang University, Hangzhou, 310018, China.*
[3]*Shaoxing Ecological Environment Pollution Prevention and Control Center, Shaoxing 310000, China.*
zjwtwaiting@hotmail.com*

(Received on 31st March 2024, accepted in revised form 12th May 2026)

Summary: In order to develop a high-efficiency adsorbent for removing trace heavy metal ions in aqueous solution, this study systematically evaluated the adsorption performance of four carbon materials. The study investigates how morphology, surface functional groups, and charge characteristics affect adsorption performance, and elucidates the dominant adsorption mechanism via modeling and thermodynamic analysis. Activated carbon and its nitrogen-modified derivative show excellent Co^{2+} adsorption ability adsorption performance with a maximum of 80%. The adsorption behavior conforms to monolayer adsorption mechanism. For activated carbon and beard-shaped carbon nanotubes, Co^{2+} removal is mainly achieved through adsorption capacity with uptake capacity correlating positively with textural properties. In contrast, adsorption of Co^{2+} by N-doped AC and OH-functionalized CNTs involves two mechanisms: physical adsorption and chemical adsorption, and its adsorption mechanism is affected by the density of the surface hydroxyl group. In five consecutive adsorption-desorption cycles, all materials maintain stable adsorption efficiency (maintained at more than 95% of the initial adsorption capacity). In the mixed metal competitive adsorption system, N-AC exhibits the highest selectivity for Pb^{2+}, followed by Co^{2+}, while Cr(VI) has the lowest adsorption capacity. It is worth noting that N-AC also shows excellent universality in removing Pb^{2+} and Cr(VI), highlighting its great application potential in the field of actual wastewater treatment.

Keywords: Heavy metal ions; Adsorbent; Activated carbon; Carbon nanotubes; Modification.

Introduction

With the continuous advancement of industrialization and the continuous expansion of economic scale, the environmental regulations and standards for wastewater discharge control and pollution control are becoming stricter and stricter. Mining, metallurgy, metal processing, electronics manufacturing and other industries continue to produce industrial wastewater containing lead, chromium, cobalt, copper and other heavy metal ions during production and operation. Such heavy metal contaminants represent a significant hazard to both ecosystem stability and public health [1-3].

Heavy metals such as Pb^{2+} and Cr(VI) are generally considered to exhibit greater acute toxicity than cobalt ion (Co^{2+}); however, given the extensive applications of Co^{2+} in fields ranging from battery manufacturing and superalloy fabrication to pigment production and electroplating processes, its discharge into the environment is increasing rapidly. Moreover, due to its high mobility in aquatic environments, Co^{2+} is often overlooked compared to traditional heavy metal pollutants. Nevertheless, even at extremely low concentrations, Co^{2+} can still be enriched in living organisms through the nutrient transfer in the food chain, which ultimately poses a potential risk to food safety and seriously affects the sustainable development of the ecological environment [4-8]. Therefore, how to efficiently remove trace heavy metals from polluted water bodies has become one of the core challenges urgently needing to be addressed in environmental field.

For the purification and treatment of heavy metal-polluted wastewater, researchers have developed a variety of physicochemical techniques, including chemical precipitation, ion exchange, membrane separation, electrochemical treatment, and adsorption [9-14]. Adsorption stands out among these methods for heavy metal removal due to its simple operation, low cost, and minimal secondary pollution. In recent years, the research and application of advanced adsorbent materials have further improved the adaptability and efficiency of adsorption in the removal of trace heavy metal ions.

*To whom all correspondence should be addressed.

Carbon-based materials have become a research hotspot in the field of heavy metal ion adsorbents due to large specific surface area, well-developed pore structure, and excellent stability, and have been widely explored and applied [15-19]. In addition to unmodified raw carbon materials, functionalized carbon materials obtained through surface modification (including nitrogen-doped carbon materials and functionalized carbon nanotubes) exhibit superior heavy metal adsorption performance through the synergistic effect of physical adsorption and surface chemical interactions [20-22]. These superior characteristics make carbon materials an ideal choice for treating heavy metal wastewater and have broad application potential in the field of environmental restoration.

Current research on carbon-based adsorbents needs to be further explored in order to advance the field. For example, under strictly controlled experimental conditions, the systematic comparative research on the adsorption mechanism of structurally heterogeneous carbon materials (such as activated carbon and carbon nanotubes) is still relatively weak. In addition, the specific mechanism of how surface functional groups (including hydroxyl and amino groups) and nitrogen-doping structures regulate the adsorption process of Co^{2+} has not been fully clarified. Building a more perfect adsorption mechanism system requires not only a deeper understanding of thermodynamic properties, but also a clearer grasp of the inherent laws followed by the adsorption behavior affected by pH value - and these key aspects are often easily ignored in existing studies. Finally, the practical application feasibility of these materials - especially their long-term stability and reusability after multiple adsorption-desorption cycles - still needs to be further verified and supported through more systematic experiments.

In order to fill the above research gaps, four representative carbonaceous materials—activated carbon (AC), nitrogen-doped modified activated carbon (N-AC), hydroxylized carbon nanotubes (HCNT) and beard-shaped carbon nanotubes (WCNT) - and used Co^{2+} as the target model pollutant. The reason why this ion was chosen is in view of the significant environmental hazards and pollution risks brought about by it in battery manufacturing, electroplating and other industrial production processes, thus highlighting the clear necessity of carrying out this research. Adsorption efficiency depends on surface area, pore structure, surface chemistry, and functional group density. In view of this, this study aims to systematically compare the adsorption capacity and mechanism through kinetics, isothermal adsorption and thermodynamic analysis; at the same time, to evaluate the influence of pH and the reusability of materials, and to examine the applicability of these materials in capturing Pb^{2+} and Cr(VI). It is expected that these research results will provide mecological understanding and design guidance for the application of carbon-based adsorbents in actual wastewater treatment.

Experimental

Experimental reagents and characterization

Experimental reagents

WCNT were purchased from Nanjing Xianfeng Nanomaterials Technology Co., Ltd. AC and HCNT were obtained from Shenzhen Suiheng Technology Co., Ltd. Cobalt nitrate, lead sulfate, potassium chromate, and melamine, all of analytical grade, were purchased from Shanghai McLin Biochemical Technology Co., Ltd. All chemicals were used as received without further purification.

Characterization Instruments

The crystallographic phases of the derived samples were characterized using a Rigaku UltimaIV X-ray diffractometer (XRD) with Cu Kα radiation, scanning from 5° to 90° at a rate of 2°/min. The morphology of the carbon materials was analyzed using a transmission electron microscope (TEM, Thermo Fisher Talos F200X G2). The presence of specific functional groups in the carbon materials was characterized by Fourier transform infrared spectroscopy (FT-IR) using a Thermo Fisher Scientific Nicolet iS20 spectrometer. N_2 adsorption-desorption experiments conducted on a Micromeritics ASAP 2460 instrument helped determine the Brunauer-Emmett-Teller (BET) surface area and pore size of the samples. Zeta potential measurements of the carbon materials were obtained using a Malvern Zetasizer Pro nanoparticle size analyzer.

Preparation of N-AC

Activated carbon/graphitic carbon nitride, referred to as N-modified activated carbon, was prepared by heating a mixture of melamine and activated carbon (Fig 1). The specific procedure is as follows: 1 g of activated carbon was ground with 20 g of melamine in a mortar for 20 min to achieve a uniform mixture. The resulting powder was then placed in a crucible and calcined in a muffle furnace at a heating rate of 823 K for 4 h. After cooling, the powder was ground for an additional 10 min to obtain the N-modified activated carbon(N-AC)[23].

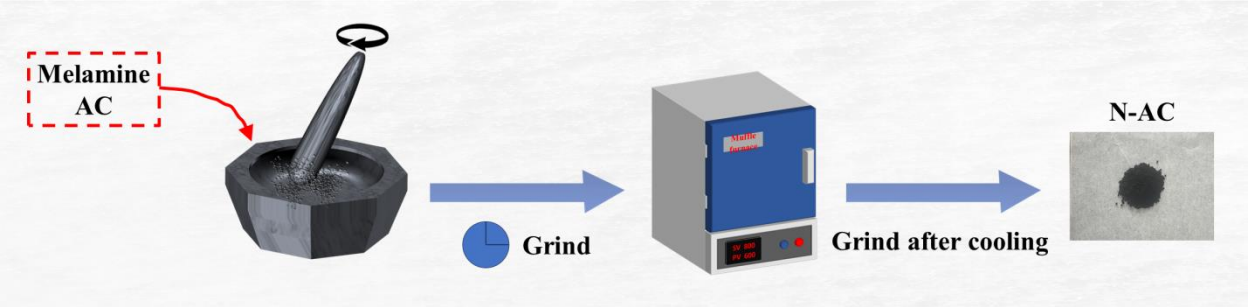

Fig. 1: Schematic diagram of N-AC preparation.

Adsorption of heavy metal ions by carbon materials

Batch adsorption experiments were conducted to collect kinetic and isotherm parameter data. In these experiments, 0.5 g of carbon material was added to 200 mL of Co^{2+} solution at a concentration of 10 mg·L^{-1}. The experimental flasks were placed in a temperature-controlled water bath set at 150 rpm to mitigate any limitations arising from the transfer of ions from the liquid to the solid phase[24]. The initial pH of the solution is 6.8±0.1, and the dissolved oxygen concentration is 5 mg·L^{-1}.

Additionally, the effects of time, temperature, and the amount of carbon material on the adsorption results were investigated. At specified time intervals, water samples were withdrawn, filtered using a 0.22 μm membrane to remove the carbon material, and then analyzed for residual metal ions using ICP.

The amount of Co^{2+} adsorbed was determined using Eq. (1):

$$q_t = \frac{(C_0 - C_t) \times v}{m} \quad (1)$$

The removal efficiency was calculated using Eq. (2):

$$R(\%) = 100 \times \frac{(C_0 - C_t)}{C_0} \quad (2)$$

where q_t represents the equilibrium adsorption capacity of the metal ions (mg·g^{-1}), C_0 and C_t are the initial concentration and the residual concentration after time t (mg·g^{-1}), respectively, m is the weight of the carbon material (g), and v is the volume of the metal ion solution (L).

Adsorption process modeling and fitting study

Carbon materials were added to Co^{2+} solutions with concentrations of 5, 10, 20, 50, and 100 mg·L^{-1}. Adsorption was conducted at room temperature for 90 min. The adsorption capacity and removal efficiency were calculated by measuring the Co^{2+} concentration after adsorption. The adsorption isotherms of the carbon materials for Co^{2+} were described using the Langmuir and Freundlich models. The Langmuir isotherm model is expressed by Eq. (3), while Eq. (4) represents the Freundlich model[25,26].

$$\frac{C_e}{q_e} = \frac{C_e}{q_m} + \frac{1}{K_\alpha q_m} \quad (3)$$

$$\ln q_e = \ln K_f + \frac{1}{n} \ln C_e \quad (4)$$

Where q_e represents the amount of pollutant adsorbed per gram of carbon material at equilibrium (mg·g^{-1}), and C_e is the equilibrium concentration of metal ions (mg·L^{-1}). q_m is the maximum adsorption capacity (mg·g^{-1}), and K_α is the Langmuir isotherm constant (L·mg^{-1}). K_f is the Freundlich constant, indicating the adsorption capacity of the carbon material at equilibrium concentration (mg$^{1-1/n}$·L$^{1/n}$·g^{-1}), while n measures the distribution of active sites on the heterogeneous surface during adsorption.

Kinetic modeling of the adsorption process

In this study, both the pseudo-first-order and pseudo-second-order adsorption kinetic models were used to describe the adsorption kinetics of Co^{2+} onto the four carbon materials, as shown in Eq. (5) and (6):

$$\ln(q_e - q_t) = \ln q_e - K_1 t \quad (5)$$

$$\frac{t}{q_t} = \frac{t}{q_e} + \frac{1}{K_2 q_e^2} \quad (6)$$

Where q_t represents the amount of pollutant adsorbed by the carbon material at time t (mg·g^{-1}), K_1 is the pseudo-first-order rate constant (min^{-1}), and K_2 is the pseudo-second-order rate constant (g·mg^{-1}·min^{-1}).

Thermodynamic analysis of the adsorption process

Adsorption thermodynamics provides valuable insights into the behavior of the process under varying temperatures. The standard Gibbs free energy (ΔG^0) and standard enthalpy (ΔH^0) can reveal the subtle differences in Co^{2+} adsorption by different carbon materials at various temperatures. These values can be calculated using Eq. (7)[27].

$$\ln K_d = \frac{\Delta S}{R} - \frac{\Delta H}{RT} \quad (7)$$

where R is the universal gas constant, with a value of 8.314 J·mol^{-1}·K^{-1}, and T is the absolute temperature in Kelvin (K). K_d represents the adsorption equilibrium constant. The relationship between lnK_d and 1/T is shown in Fig 8a.

Results and Discussion

Structure of different carbon materials

Fig 2 shows the transmission electron microscopy (TEM) images of the four carbonaceous materials studied in this paper. Both AC and N-AC show irregular layered and flaky microstructures, which is a typical feature of the skeleton structure of high porosity carbon-based materials. In stark contrast to this, HCNT and WCNT both show the unique tubular microstructure of carbon nanotubes, among which the tube diameter of HCNT is relatively small.

Textural properties (specific surface area, pore structure, and pore size distribution) are key to adsorption performance [17]. Fig 3a shows that both AC and N-AC conform to the isotherm characteristics of type I nitrogen adsorption, and show a significant H4 lag ring under high relative pressure. This characterization result shows that both materials have a composite pore structure in which micropores and mesopores coexist, which is suitable for adsorbing pollutants of different sizes. In contrast, the nitrogen adsorption-desorption isotherm of HCNT and WCNT shows typical IV-type characteristics. Combined with the lag ring morphology of the isotherm, it can be seen that these two materials have a mixed structure of microporous and mesoporous, and have good pore connection [28]. The aperture distribution curve (Fig 3b) further confirms the above conclusion: the aperture distribution range of AC and HCNT is relatively wide and can accommodate metal ions of various sizes; while N-AC and WCNT are mainly characterized by tiny pore structures. Based on the BET method, the specific surface area of AC and N-AC is 1285.5 m^2·g^{-1} and 1837.4 m^2·g^{-1} respectively, both of which are significantly higher than the typical values of traditional carbon-based adsorbents. This high specific surface area characteristic can effectively provide sufficient active sites for the adsorption of metal ions and significantly reduce the mass transfer resistance of adsorbents, thus playing an important role in improving the adsorption performance [17].

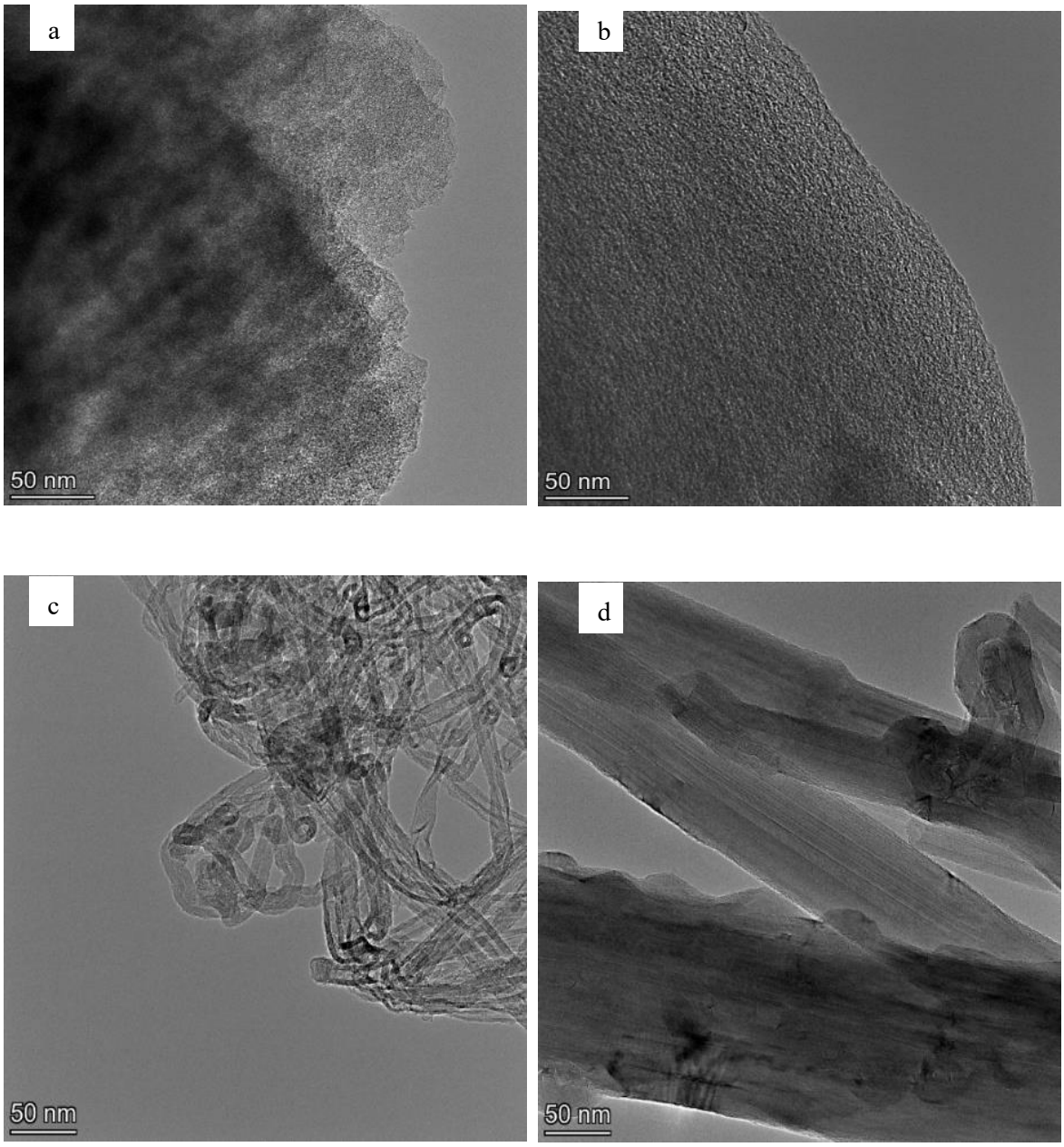

Fig. 2 TEM images of four carbonaceous materials

(a) AC showing irregular layered and flaky microstructures; (b) N-AC showing a typical porous carbon skeleton with layered morphology; (c) HCNT showing a tubular microstructure; (d) WCNT showing a tubular morphology

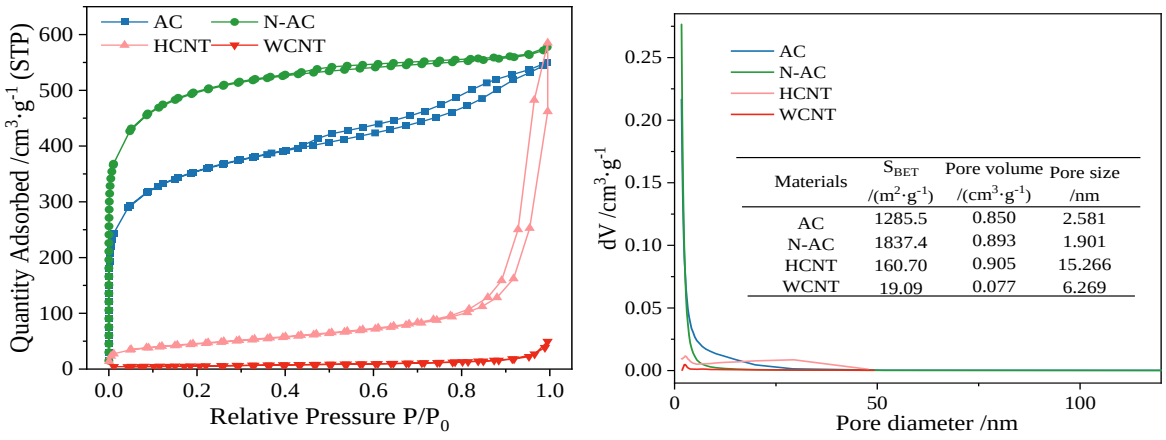

Fig. 3: N_2 adsorption/desorption curve (a) and pore size distribution (b)

The interaction between carbon-based materials and heavy metal ions is not only strongly regulated by the specific surface area and pore structure and other texture characteristics, but also affected by crystallographic characteristics and surface chemical function groups - these factors are particularly critical in determining chemical adsorption behavior. In order to systematically clarify the differences in the structural characteristics of these four carbon materials, this study carried out XRD (X-ray diffraction) and FT-IR (Fourier transform infrared spectrum) characterization. The XRD spectrum shows that AC (activated carbon) and N-AC (nitrogen-doped activated carbon) do not show obvious characteristic diffraction peaks (Fig 4a). This characterization result shows that the carbon skeleton of these two materials mainly has an amorphous structure and low crystallinity. In stark contrast, HCNT and WCNT both present clear and sharp characteristic diffraction peaks at positions of about 26°and 43° at 2θ angles. The peaks at ≈26° and 43° belong to the (002) and (100) crystal surfaces of graphitized carbon. This is a typical graphite crystal structure feature of carbon nanotube materials, indicating that both materials have high crystallinity [29].

In the FT-IR spectra of all four carbon samples, a wide absorption peak appeared at 3419 cm^{-1} (Fig 4b), which belongs to O-H expansion vibration, confirming the presence of hydroxyl groups on its surface [30]. It is worth noting that the absorption peak intensity of N-AC and HCNT here is significantly higher than that of AC and WCNT, indicating that the abundance of the surface-OH functional groups of the first two is higher, which is conducive to promoting the complex reaction between metal and the surface of the material. The absorption peaks at 1633 cm^{-1} and 1129 cm^{-1} correspond to the bending vibration pattern of –NH [30]. Overall, the above results fully reveal that there are significant differences in crystallinity and surface chemical properties of these four carbon materials, and these differences are expected to have a strong regulatory effect on their adsorption behavior.

Co^{2+}uptake by carbon-based materials under different operational conditions

Under the condition that the adsorbent addition is 2.5 $g·L^{-1}$ and the concentration of Co^{2+} is 10 $mg·L^{-1}$, Fig 5a shows the removal efficiency of Co^{2+} of four carbon materials and the time required to achieve adsorption equilibrium. All materials show rapid adsorption properties, and adsorption equilibrium can be achieved in about 30 min, and then until 90 min, the removal efficiency is basically constant. Under the same experimental conditions, the

adsorption of N-AC and AC on Co^{2+} is significantly higher than that of the other two materials based on carbon nanotubes. This performance improvement is mainly due to its large specific surface area and high porosity. Among the tested adsorbents, N-AC showed the highest removal efficiency; when the adsorption equilibrium was reached, its removal rate of Co^{2+} exceeded 70%. For the four carbon-based materials selected in this study, increasing the amount of adsorbent within a certain range can significantly improve the removal effect of Co^{2+}. The fundamental reason is that increasing the amount of adsorbent will proportionally increase the density of active adsorption sites in the system, so that Co^{2+} ions in the solution can be more fully captured. However, the experimental results show that when the concentration of adsorbent increases to more than 2.5 $g \cdot L^{-1}$, the improvement of the removal effect of these four materials on Co^{2+} is negligible. This trend shows that the adsorption active site in the system has basically reached saturation; in addition, the further improvement of removal efficiency may also be constrained by secondary factors such as increased mass transfer resistance in the solution and aggregation of adsorbent particles [24]. Considering the standard requirements of Co^{2+} removal performance and the economic cost control needs in practical engineering applications, this study finally determined that 2.5 $g \cdot L^{-1}$ was the best adsorbent addition for all subsequent adsorption experiments.

The influence of temperature on Co^{2+} uptake by carbon materials was systematically examined across three temperature settings under previously determined optimal adsorbent loading. The relevant test results are summarized in Fig 5c. The removal efficiency of Co^{2+} by the four carbon-based materials showed a continuous decreasing trend with the gradual increase of the reaction system temperature (Fig 5c). This result clearly indicates a close correlation between the adsorption process and the temperature factor. The significant decrease in adsorption capacity at high temperatures further corroborates that The uptake of Co^{2+} by the selected carbon-based materials is predominantly exothermic in nature.

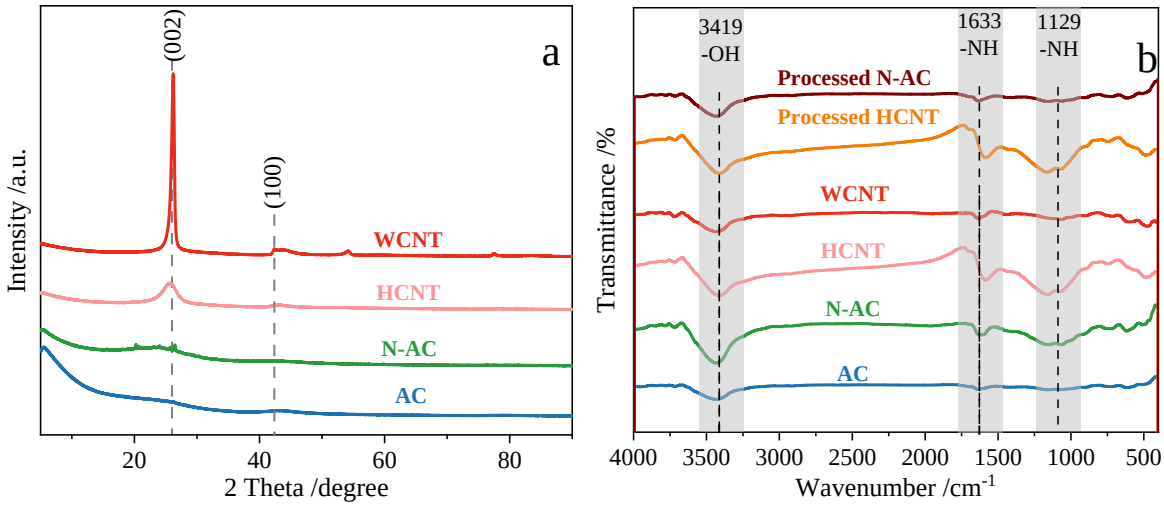

Fig. 4 XRD patterns (a) and FT-IR spectra (b) of four carbonaceous materials

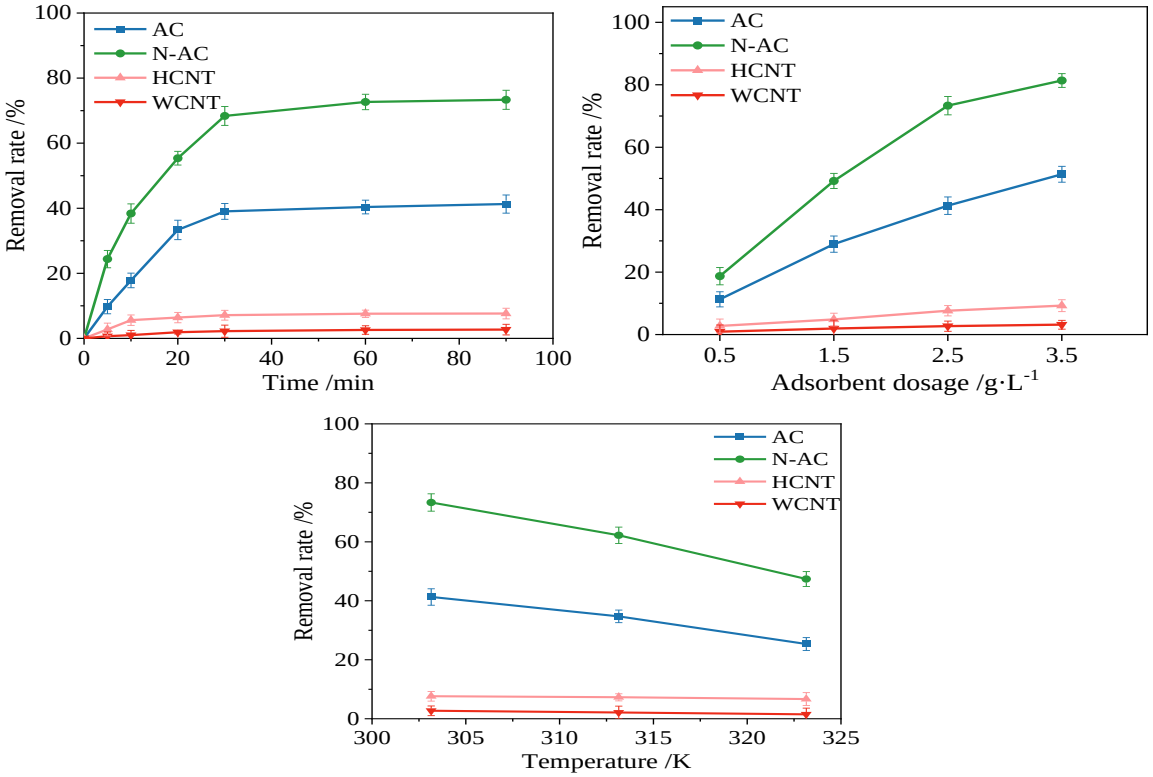

Fig. 5 Influences of time (a), dose (b), and temperature (c) on Co^{2+} removal by four carbonaceous materials

Adsorption curve fitting for Co^{2+} uptake on carbon materials

Equilibrium data for Co^{2+} adsorption on the carbon materials were fitted with Langmuir and Freundlich isotherms (Fig 6), with the resulting parameters summarized in Table 1. For the four materials tested, the Langmuir isotherm consistently outperformed the Freundlich model, giving higher R^2 values and i better fit. This suggests Co^{2+} adsorption mainly carried out through a single-layer covering mechanism, and the interaction between adsorption ions is negligible [17].

Table-1: Adsorption isothermal model fitting parameters.

Carbon materials	temperatures /K	Langmuir model			Freundlich model		
		q_m/mg·g^{-1}	K_a/L·mg^{-1}	R^2	K_f /mg$^{1-1/n}$·L$^{1/n}$·g^{-1}	1/n	R^2
AC	303.15	4.512	0.114	0.995	0.937	0.351	0.981
	313.15	3.663	0.100	0.991	0.747	0.346	0.982
	323.15	2.964	0.079	0.996	0.488	0.390	0.984
N-AC	303.15	9.995	0.329	0.999	2.672	0.357	0.944
	313.15	8.703	0.152	0.999	1.546	0.436	0.917
	323.15	7.034	0.086	0.997	0.877	0.491	0.917
HCNT	303.15	1.134	0.052	0.991	0.116	0.482	0.941
	313.15	1.053	0.050	0.990	0.115	0.468	0.939
	323.15	0.995	0.048	0.990	0.099	0.488	0.941
WCNT	303.15	0.376	0.056	0.992	0.038	0.489	0.921
	313.15	0.277	0.051	0.988	0.028	0.503	0.891
	323.15	0.229	0.047	0.992	0.020	0.507	0.929

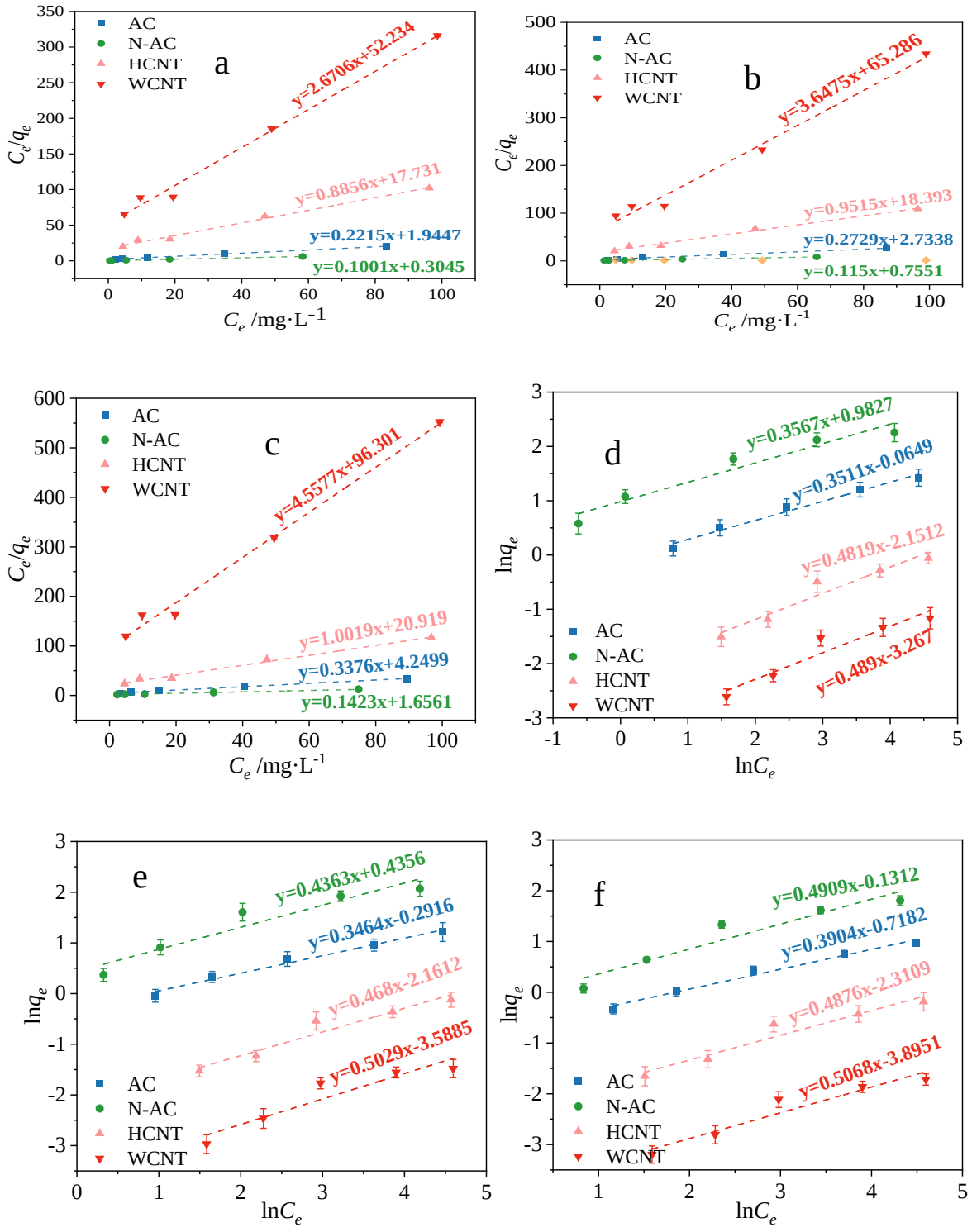

Fig. 6 Langmuir(a~c)and Freundlich(d~f) models of four carbon materials a&d. 303.15K; b&e. 313.15K; c&f. 323.15K

To evaluate the adsorption performance of the materials, we compiled Table 2, which compares the q_m values of the four carbon materials we prepared for Co^{2+} with the corresponding values reported in the literature for various carbon-based and other adsorbents. Among the listed studies, N-AC had the highest q_m value, approximately 10.0 mg · g^{-1}, which was lower than many previously reported carbon based adsorbents (Table 2). This is primarily attributed to its high specific surface area and the surface functional groups induced by nitrogen doping. This indicates that N-AC is a promising candidate for the removal of Co^{2+} from aqueous solutions.

Table-2: Comparison of q_m for Co^{2+} removal by various adsorbents.

Carbon materials	q_m (mg·g^{-1})	Conditions		Reference
		pH	T (K)	
AC	**4.512**	**6.8**	**303.15**	**This work**
N-AC	**9.995**	**6.8**	**303.15**	**This work**
HCNT	**1.134**	**6.8**	**303.15**	**This work**
WCNT	**0.376**	**6.8**	**303.15**	**This work**
Oxidized CNTs	**1.45**	**7.0**	**298**	**[8]**
MWCNTs/iron oxide	**0.82**	**6,4**	**298**	**[8]**
Eggshells	**2.99**	**7.0**	**298**	**[31]**
MWCNT/PPY/$NaBH_4$	**2.11**	**7.0**	**298.15**	**[31]**

Comparison of the kinetics of Co^{2+} adsorption on carbon materials

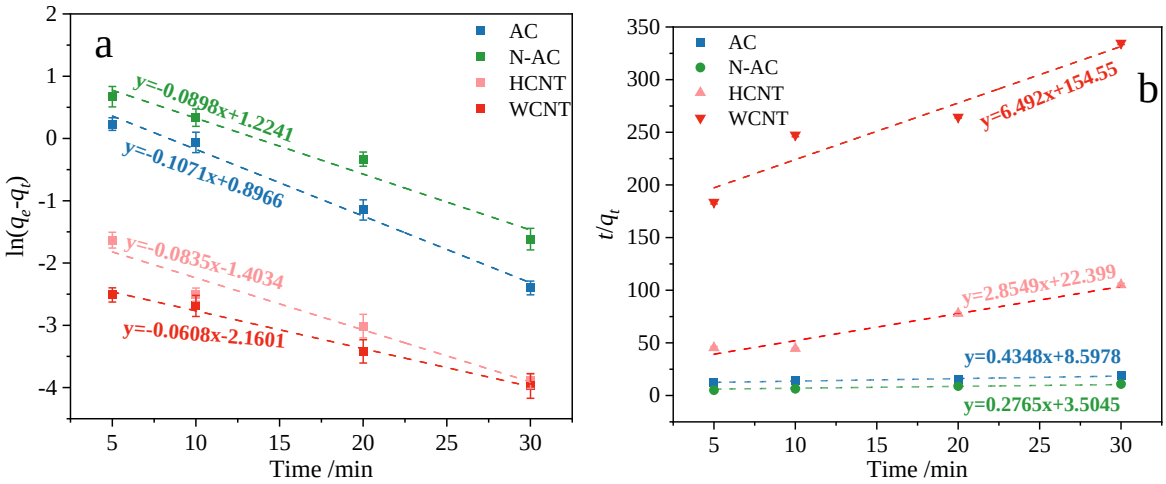

Fig. 7: Adsorption kinetics model of pseudo-first-level (a) and pseudo-second-level (b) of four carbon materials.

The dynamic fitting results obtained using the applied model are presented in Fig 7, a Table 3 lists the fitted parameters along with the corresponding R^2 values. For AC and WCNT, the pseudo-first-level model can better describe the experimental data. Its R^2 values are 0.989 and 0.992 respectively, both of which are higher than the values obtained by the pseudo-second-level model (0.950 and 0.982). In contrast, the adsorption kinetics of N-AC and HCNT fits the pseudo-secondary model. The high degree of coincidence between the equilibrium adsorption amount qe obtained and the experimental value further confirms this difference. Physical adsorption governs Co^{2+} uptake by AC and WCNT, with adsorption capacity correlating primarily with specific surface area and pore volume [17]. Because its specific surface area is significantly larger than WCNT, AC shows a higher Co^{2+} adsorption amount. On the contrary, the

adsorption behavior of N-AC and HCNT involves the synergy of physical and chemical interactions. For such systems, both the material's structural features and the density of surface hydroxyl groups (among other functionalities) influence adsorption capacity [17]. Among these four materials, N-AC shows the highest Co^{2+} adsorption performance; A synergistic high surface activity accounts for this observation.

To gain direct insight into the interactions between Co^{2+} and surface functional groups, we recorded the FT-IR spectra of N-AC and HCNT after the adsorption of Co^{2+} (Fig. 4b). Both the O–H stretching vibration peak located at approximately 3419 cm^{-1} and the N–H bending vibration peak located at approximately 1633 cm^{-1} exhibited a distinct shift toward lower wavenumbers, accompanied by a decrease in peak intensity; this indicates the formation of Co–O and Co–N coordination complexes. These findings corroborate the results obtained from the kinetic models.

Thermodynamic comparison of carbon material adsorption Co^{2+} process

Table 4 presents the main thermodynamic parameters for Co^{2+} adsorption on four carbon-based materials, notably including ΔH^0 and ΔG^0. The calculation results of the experimental data show that the ΔH^0 value of all measured carbon-based adsorbents is negative. The exothermic nature of Co^{2+} adsorption on these four carbon surfaces is supported by the thermodynamic data. This conclusion is highly consistent with the phenomenon observed in the above temperature effect experiment - that is, "temperature increase leads to a significant decrease in Co^{2+} removal efficiency" - which achieves mutual verification between thermodynamic theoretical analysis and experimental phenomena, and further consolidates the reliability of the conclusion of this study. Temperature-dependent changes in ΔG^0 offer an important criterion for judging adsorption system thermal stability. its numerical fluctuation directly reflects the sensitivity of the adsorption process to temperature fluctuations. Among the four carbon-based materials selected in this study, HCNT shows the best thermal stability: when the temperature of the reaction system rises by 10 K (from 303.15 K to 313.15 K), the attenuation rate of its adsorption capacity is less than 10%; while AC, N-AC and W The adsorption capacity of CNT has decreased by more than 20%, and its thermal stability is significantly inferior to that of HCNT. The excellent thermal stability shown by HCNT is speculated to be closely related to its unique surface chemical composition and structural characteristics, especially the hydroxyl groups enriched on its surface. Hydroxyl groups can significantly enhance the intensity of interaction between the adsorbent and the surface of the adsorbent by complexing with Co^{2+}, thus effectively alleviating the negative impact of temperature fluctuations on the adsorption process. Among the above four materials, the absolute value of ΔH^0 of HCNT is the lowest, which indicates that it releases relatively little heat in the process of adsorption of Co^{2+}. This mild enthalpy characteristic can be regarded as one of the key intrinsic reasons why HCNT is insensitive to temperature changes and shows excellent thermal stability.

Table-3: Parameters derived from adsorption kinetic modeling.

Carbon materials	Pseudo-first-order kinetic model			Pseudo-second-order kinetic model		
	q_e/(mg·g^{-1})	K_1/(min^{-1})	R^2	q_e/(mg·g^{-1})	K_2/(g·mg^{-1}·min^{-1})	R^2
AC	**2.451**	**0.107**	**0.989**	**2.300**	**0.022**	**0.950**
N-AC	**3.401**	**0.090**	**0.971**	**3.610**	**0.022**	**0.994**
HCNT	**0.084**	**0.248**	**0.959**	**0.350**	**0.364**	**0.992**
WCNT	**0.115**	**0.061**	**0.992**	**0.154**	**0.273**	**0.982**

Table-4: Carbonaceous materials: derived thermodynamic parameters.

Carbon materials	ΔH^0/(KJ·mol^{-1})	ΔG^0/(KJ·mol^{-1})		
		303.15 K	313.15 K	323.15K
AC	-14.59	-1.701	-1.276	-0.850
N-AC	-54.70	-4.268	-2.604	-0.941
HCNT	-3.140	0.328	0.442	0.556
WCNT	-6.760	0.139	0.367	0.595

Extended Applications of Various Carbon Materials for Heavy Metal Adsorption

Reuse Potential of Carbon Materials for Heavy Metal Ion Uptake

Reusability represents a core indicator for evaluating the feasibility of practical engineering applications of carbon-based adsorbents. The key reason is that optimizing the regeneration performance of the adsorbent can significantly reduce the operating costs and resource consumption of such materials in large-scale heavy metal wastewater treatment scenarios [32,33]. To systematically evaluate the recycling potential of the four carbon-based materials selected in this study, five consecutive cycles of adsorption-desorption stability experiments were designed and conducted. After each adsorption cycle, the saturated and exhausted adsorbent was first separated by filtration, and then immersed in a 0.1 M HCl solution for desorption regeneration. The desorption process was carried out at room temperature, while being continuously stirred in a shaker at a constant speed of 150 rpm for 120 min to ensure that the Co^{2+} adsorbed on the material surface was fully desorbed. After the desorption operation, the regenerated carbon material was repeatedly rinsed with deionized water until the pH of the washing solution reached neutral, and then placed in an 80℃ constant temperature oven to dry for 12 h. After the material was completely dry, it was used for the next round of adsorption experiments. The Co^{2+} removal performance was largely maintained across five successive adsorption-desorption cycles, without significant degradation. This fully demonstrates that the selected carbon-based materials possess excellent structural stability and efficient regeneration performance. These research results further highlight the great application potential and engineering value of carbon-based adsorbents, especially AC and N-AC activated carbon materials, for reuse in actual heavy metal wastewater treatment systems.

Adsorption characteristics of carbon materials toward diverse heavy metal ions

For systematically evaluating the practical application potential of the four carbon-based materials selected in complex heavy metal-contaminated water bodies, and to clarify their adsorption selectivity and universality for heavy metal pollutants of different valence states and types, this study selected the typical and common pollutants Pb^{2+} and Cr(VI) in the water environment as characteristics. Standard pollutants, as shown in Fig 9, compared with the removal efficiency of Cr(VI), these four carbon-based adsorbents have a higher removal efficiency for Pb^{2+}.The essence of this phenomenon is attributed to the fundamental differences in the existence form and charge characteristics of the two heavy metal ions in the experimentally set aqueous solution system. Specifically, in the solution environment controlled in this experiment, Cr(VI) mainly exists stably in the form of negatively charged chromate ions (CrO_4^{2-}) [34,35], while Pb^{2+} is positively charged cations.

To further substantiate the rationality of the above adsorption mechanism, this study simultaneously conducted Zeta potential characterization tests. The four carbon-based materials all exhibited stable negative surface charges. The negative charge characteristics of the adsorbent surface can generate strong electrostatic attraction with positively charged metal ions in the solution, thereby significantly enhancing the binding effect between the adsorbate and the adsorbent surface. Based on this, it can be inferred that the stronger electrostatic interaction between Pb^{2+} and the carbon-based material surface is the core dominant factor that makes its adsorption efficiency significantly higher than Cr(VI); while the negatively charged CrO_4^{2-} significantly inhibits the effective adhesion and enrichment process of Cr(VI) on the adsorbent surface, ultimately leading to its lower removal efficiency.

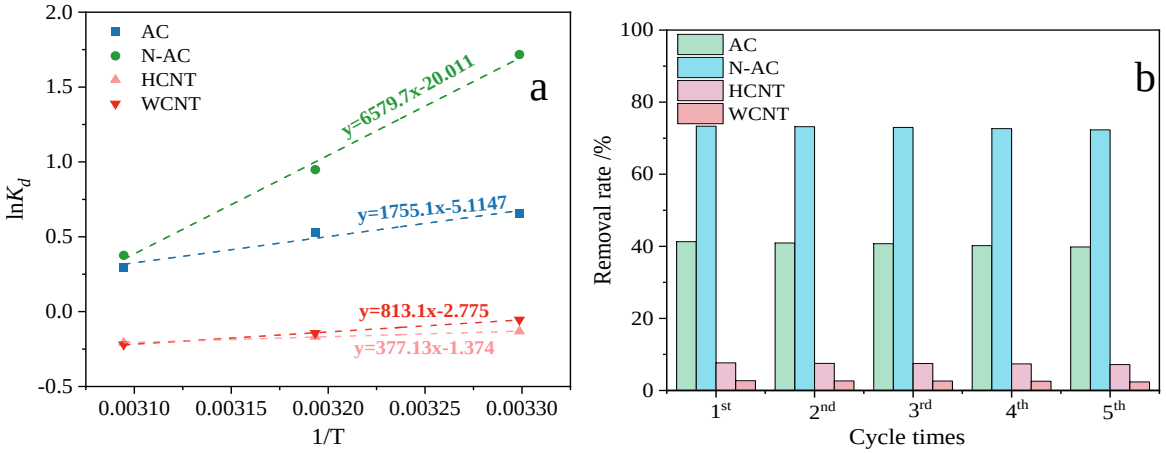

Fig. 8 Relationship between lnK_d and 1/T (a) and repeatability verification (b)

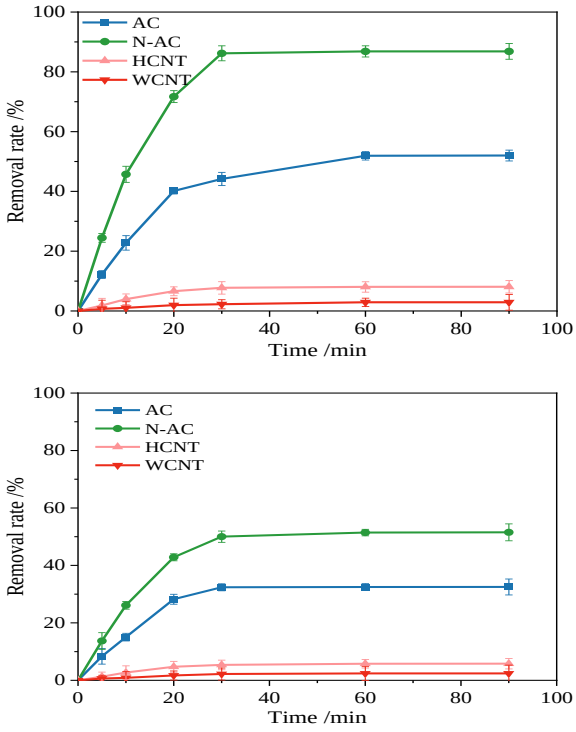

Fig. 9: Uptake of Pb^{2+} (a) and Cr(VI) (b) onto four carbon-based adsorbents.

Selectivity of carbon materials toward heavy metal ions in mixed systems

To evaluate the selective adsorption performance of four carbon materials in an environment where Pb^{2+}, Co^{2+}, and Cr(VI) coexist, we conducted competitive adsorption experiments [36]. As shown in Table 5, N-AC has the highest selectivity for Pb^{2+}, followed by Co^{2+}, and the lowest selectivity for Cr(VI). Meanwhile, AC and WCNT exhibit moderate selectivity towards Pb^{2+}. The selectivity of HCNT is not significant, but its adsorption capacity for Pb^{2+} is still superior to Co^{2+} and Cr(VI). This selective sequence is consistent with the electrostatic interaction mechanism previously described. Compared with Co^{2+}, Pb^{2+}has higher selectivity, which can be attributed to its smaller hydrated ion radius.

Table-5: Competitive adsorption removal efficiencies of four carbon materials in mixed metal ion system.

Carbon material	Co^{2+} removal (%)	Pb^{2+} removal (%)	Cr(VI) removal (%)
AC	38.6	62.4	6.3
N-AC	41.5	68.3	8.7
HCNT	12.4	23.7	3.2
WCNT	8.9	18.9	2.1

Conclusions

This study systematically evaluated the adsorption performance of four carbon materials: AC, N-AC, HCNT, and WCNT - to remove Co^{2+} from aqueous solution. Among them, N-AC shows the highest adsorption capacity, and its removal efficiency exceeds 70% under optimized conditions; followed by AC; while the adsorption performance of HCNT and WCNT is relatively low. The adsorption process is well described by the Langmuir isotherm model; based on thermodynamic research, the process is determined to be a spontaneous and heat-emitting reaction. Co^{2+} adsorption by AC and WCNT is primarily physical in nature, closely relating to the specific surface area and pore structure of the materials. In contrast, the adsorption process of N-AC and HCNT involves the synergy of physical adsorption and chemical adsorption, and is closely related to the density of hydroxyl groups and other functional groups on the surface of the material. All the tested materials showed excellent reusability. After five consecutive adsorption-desorption cycles, their adsorption capacity can still be maintained at more than 95% of the initial value. In addition, N-AC shows significant adsorption ability on Pb^{2+}, but its adsorption performance on Cr(VI) is relatively limited due to

unfavorable electrostatic interaction. The competitive adsorption experiment further confirmed that the selective order is determined by electrostatic interactions. These research results highlight the decisive influence of surface characteristics on adsorption behavior, and establish the potential value of N-AC as a highly promising and versatile adsorbent in removing heavy metal ions in actual wastewater treatment.

Acknowledgment

We would like to express our sincere gratitude to the Natural Science Foundation of Zhejiang Province (Contracts LY19B060004) for supporting this study.

Funding

This work was supported by the National Natural Science Foundation of China (Grant No. 51876038).

References

2. Arshad, F., Al Momani, D. E., de Vos, W. M., Zou, L., Nanocomposite membrane for simultaneous removal of dye and heavy metal ions from wastewater. *J. Environ. Manage.*, **371**, 123242(2024).
3. Kumar, A., Thakur, A., Panesar, P. S., A review on the industrial wastewater with the efficient treatment techniques. *Chem. Pap.*, **77**, 4131–4163(2023).
4. Azimi, A., Azari, A., Rezakazemi, M., Ansarpour, M., Removal of heavy metals from industrial wastewaters: A review. *ChemBioEng Rev.*, **4**, 37–59(2017).
5. Yi, X., Ullah, N., Zhao, Q., Xiao, J., Zhang, N., Li, S.-L., Hu, Y., Gong, G., Fabrication of tight polyamide nanofiltration membrane by using a pyridine-diamine precursor for heavy metal ions removal. *Sep. Purif. Technol.*, **358**, 130424(2025).
6. Bjørklund, G., Semenova, Y., Pivina, L., Dadar, M., Rahman, Md. M., Aaseth, J., Chirumbolo, S., Uranium in drinking water: a public health threat. *Arch. Toxicol.*, **94**, 1551–1560(2020).
7. Verma, B., Balomajumder, C., Surface modification of one-dimensional carbon nanotubes: a review for the management of heavy metals in wastewater. *Environ. Technol. Innovation*, **17**, 100596(2020).
8. Zhang, J., Li, T., Li, X., Liu, Y., Li, N., Wang, Y., Li, X., A key role of inner-cation-π interaction in adsorption of pb(II) on carbon nanotubes: experimental and DFT studies. *J. Hazard. Mater.*, **412**, 125187(2021).
9. Xu, J., Cao, Z., Zhang, Y., Yuan, Z., Lou, Z., Xu, X., Wang, X., A review of functionalized carbon nanotubes and graphene for heavy metal adsorption from water: preparation, application, and mechanism. *Chemosphere*, **195**, 351–364(2018).
10. Hundessa, N. K., Hu, C.-C., Kang, D.-Y., Ajebe, E. G., Habet, B. A., Hung, W.-S., Lee, K.-R., Lai, J.-Y., A novel trimesoyl chloride/hyper branched polyethyleneimine/MOF (MIL-303)/P84 co-polyimide nanocomposite mixed matrix membranes with an ultra-thin surface cross linking layer for removing toxic heavy metal ions from wastewater. *J. Hazard. Mater.*, **480**, 136221(2024).
11. Swathe Sriee, A. E., Shankar, V., Three-dimensional bioprinted materials in alginate-hyaluronic acid complex based hydrogel based bio-ink as absorbents for heavy metal ions removal. *Carbohydr. Polym. Technol. Appl.*, **8**, 100588(2024).
12. Han, M., Shen, X., Zhang, G., Liu, Y., Zhai, Y., Highly recyclable magnetic Fe_3O_4@CSH derived from industrial silicon residue: Application in heavy metal ion adsorption. *J. Water Process Eng.*, **68**, 106412(2024).
13. Feisal, N. A. S., Kamaludin, N. H., Ahmad, M. A., Tengku Ibrahim, T. N. B., A comprehensive review of nanomaterials for efficient heavy metal ions removal in water treatment. *J. Water Process Eng.*, **64**, 105566(2024).
14. Dhokpande, S. R., Deshmukh, S. M., Khandekar, A., Sankhe, A., A review outlook on methods for removal of heavy metal ions from wastewater. *Sep. Purif. Technol.*, **350**, 127868(2024).
15. Li, J., Wang, X., Zhao, G., Chen, C., Chai, Z., Alsaedi, A., Hayat, T., Wang, X., Metal–organic framework-based materials: superior adsorbents for the capture of toxic and radioactive metal ions. *Chem. Soc. Rev.*, **47**, 2322–2356(2018).
16. Habibi, R., Barzegar, B., Aghdasinia, H., Khataee, A., Enhancement of filtration performance and antifouling properties of polyethersulfone membranes using Fe_3O_4@walnut shell-derived activated carbon nanocomposite for heavy metal ions removal. *J. Environ. Chem. Eng.*, **12**, 113172(2024).
17. Radwan, O. H., Nusseir, A. M., Ghanem, M. A., Mostafa, N. Y., Mohammed, K. M. H., Abou El-Nour, K. M., Magnetic sodium titanate nanotubes for simultaneous recovery of multiple low-level heavy and radioactive metal ions. *Inorg. Chem. Commun.*, **167**, 112773(2024).
18. Sheraz, N., Shah, A., Haleem, A., Iftikhar, F. J., Comprehensive assessment of carbon-, biomaterial- and inorganic-based adsorbents for the removal of the most hazardous heavy metal ions from wastewater. *RSC Adv.*, **14**, 11284–11310(2024).
19. Wang, T., Ling, C., Si, Y., Li, L., Xing, B., Fabrication of a graphitic N-doped *sp2/sp3* carbon

interface in carbon-based materials for efficient removal of antibiotics. *Chem. Eng. J.*, *513*, 162770(2025).

20. Sánchez-Yepes, A., Ferreira, A. P., Santos, A., Romero, A., Gomes, H. T., Lorenzo, D., Novel carbon-based materials for sustainable water treatment: perfluorooctanoic acid adsorption and adsorbent regeneration via thermally activated persulfate oxidation. *J. Environ. Chem. Eng.*, **13**, 120084(2025).
21. Wang, F., Hou, L., Aryee, A. A., Rashda, Ma, Y., Qu, L., Han, R., Adsorption and catalytic degradation of malachite green by polyethyleneimine modified HO-CNTs/$CuNiFe_2O_4$. *Inorg. Chem. Commun.*, **181**, 115210(2025).
22. Mishra, S. R., Gadore, V., Singh, K. R., Pandey, S. S., Ahmaruzzaman, Md., Developing In_2S_3 upon modified $MgTiO_3$ anchored on nitrogen-doped CNT for sustainable sensing and removal of toxic insecticide clothianidin. *Environ. Res.*, **259**, 119435(2024).
23. Wang, X., Mo, Y., Deng, X., Cai, Y., Guo, C., Chen, J., Wang, W., Li, G., Multifunctional nitrogen-doped graphene quantum dots enables efficient and stable GaAs/CNT heterojunctions solar cell. *Carbon*, **243**, 120535(2025).
24. Lu, S., Liu, F., Qiu, P., Qiao, M., Li, Y., Cheng, Z., Xue, N., Hou, X., Xu, C., Xiang, Y., Peng, F., Guo, Z., Photothermal-assisted photocatalytic degradation with ultrahigh solar utilization: Towards practical application. *Chem. Eng. J.*, **379**, 122382(2020).
25. Li, K., Chen, M., Chen, L., Zhao, S., Pan, W., Li, P., Han, Y., Adsorption of tetracycline from aqueous solution by ZIF-8: Isotherms, kinetics and thermodynamics. *Environ. Res.*, **241**, 117588(2024).
26. Xu, J., Lv, X., Li, J., Li, Y., Shen, L., Zhou, H., Xu, X., Simultaneous adsorption and dechlorination of 2,4-dichlorophenol by Pd/Fe nanoparticles with multi-walled carbon nanotube support. *J. Hazard. Mater.*, **225–226**, 36–45(2012).
27. Andersson, K. I., Eriksson, M., Norgren, M., Removal of lignin from wastewater generated by mechanical pulping using activated charcoal and fly ash: adsorption isotherms and thermodynamics. *Ind. Eng. Chem. Res.*, **50**, 7722–7732(2011).
28. Lima, E. C., Hosseini-Bandegharaei, A., Moreno-Piraján, J. C., Anastopoulos, I., A critical review of the estimation of the thermodynamic parameters on adsorption equilibria. wrong use of equilibrium constant in the van't hoof equation for calculation of thermodynamic parameters of adsorption. *J. Mol. Liq.*, **273**, 425–434(2019).
29. Salatein, Nahla. M., Shaaban, M., Fahim, Irene. S., Comparing low-cost activated carbon made from coffee waste and bagasse to remove heavy metals and methylene blue dye. *Results Chem.*, **13**, 102020(2025).
30. Ton-That, L., Nguyen, T.-P.-T., Duong, B.-N., Nguyen, D.-K., Nguyen, N.-A., Ho, T., Dinh, V.-P., Insights into Pb (II) adsorption mechanisms using jackfruit peel biochar activated by a hydrothermal method toward heavy metal removal from wastewater. *Biochem. Eng. J.*, **212**, 109525(2024).
31. Wang, Z., Xiang, B., Cheng, R., Li, Y., Behaviors and mechanism of acid dyes sorption onto diethylenetriamine-modified native and enzymatic hydrolysis starch. *J. Hazard. Mater.*, **183**, 224–232(2010).
32. Rethinasabapathy, M., Ghoreishian, S. M., Kwak, C. H., Han, Y.-K., Roh, C., Huh, Y. S., Recent progress in advanced functional materials for adsorption and removal of cobalt from industrial and radioactive effluents. *Coord. Chem. Rev.*, **527**, 216401(2025).
33. Alhammadi, Y., Hai, A., Taher, H., Banat, F., AlMarzooqi, F., Enhancing heavy metals filtration: synergistic effects of banana peel-derived activated carbon and layered double hydroxides in ultrafiltration membranes. *Sep. Purif. Technol.*, **362**, 131875(2025).
34. Shen, C., Sun, K., Yang, Y., Liu, C., Liu, Y., Wang, X., Photoreductive elimination of heavy metal ions and radionuclides by g-C_3N_4-based materials: a review. *Sep. Purif. Technol.*, **363**, 132023(2025).
35. Ravindiran, G., Rajamanickam, S., Ramalingam, M., Hayder, G., Sathaiah, B. K., Gaddam, M. K. R., Muniasamy, S. K., Arunkumar, P., Conversion of seaweed waste to biochar for the removal of heavy metal ions from aqueous solution: A sustainable method to address eutrophication problem in water bodies. *Environ. Res.*, **241**, 117551(2024).
36. Kobya, M., Demirbas, E., Senturk, E., Ince, M., Adsorption of heavy metal ions from aqueous solutions by activated carbon prepared from apricot stone. *Bioresour. Technol.*, **96**, 1518–1521(2005).
37. Ding, R., Lu, J., Zhang, X., Phthalocyanine and amine cofunctionalized porous organic polymer for selective gold recycling from electronic waste. *ACS Sustainable Chem. Eng.*, **13**, 12625–12633(2025).